Journal of Chromatography B, 913–914 (2013) 129–136

Contents lists available at SciVerse ScienceDirect

Journal of Chromatography B

journal homepage: www.elsevier.com/locate/chromb

Sensitive method for plasma and tumor Ko143 quantification using reversed-phase high-performance liquid chromatography and fluorescence detection

Serge A.L. Zander[a], Jos H. Beijnen[b,c,d], Olaf van Tellingen[e,*]

[a] Division of Molecular Oncology, The Netherlands Cancer Institute, Plesmanlaan 121, 1066 CX Amsterdam, The Netherlands
[b] Department of Pharmacy and Pharmacology, Slotervaart Hospital, Louwesweg 6, 1066 EC Amsterdam, The Netherlands
[c] Faculty of Science, Department of Pharmaceutical Sciences, Division of Pharmacoepidemiology & Clinical Pharmacology, Utrecht University, Universiteitsweg 99, 3584 CG Utrecht, The Netherlands
[d] Department of Clinical Pharmacology, The Netherlands Cancer Institute, Plesmanlaan 121, 1066 CX Amsterdam, The Netherlands
[e] Department of Clinical Chemistry, The Netherlands Cancer Institute, Plesmanlaan 121, 1066 CX Amsterdam, The Netherlands

ARTICLE INFO

Article history:
Received 3 May 2012
Accepted 5 November 2012
Available online 6 December 2012

Keywords:
Ko143
Fumitremorgin C
Roquefortine C
Topotecan
ABCG2
Drug resistance

ABSTRACT

The fumitremorgin C analogue Ko143 is a potent and selective inhibitor of the ATP-binding cassette transporter ABCG2. To support *in vivo* ABCG2 resistance studies, we developed a sensitive and selective method for Ko143 quantification in plasma and tumor samples, using the parent compound fumitremorgin C as internal standard. Sample pretreatment by liquid–liquid extraction in diethyl ether yielded a recovery of 50% from human and mouse plasma. Pretreated samples were separated by reversed-phase high-performance liquid chromatography with fluorescence detection at 295 nm excitation and 350 nm emission wavelengths. Sharp chromatographic peaks were obtained with a 5 μm GraceSmart C18 column. The mobile phase consisted of methanol:10 mM ammonium acetate pH 5.0 (62:38, v/v), delivered at a flow rate of 0.2 mL/min. Acceptable accuracy and precision of ±15% were achieved within the linear dynamic range of the calibration curve (2–500 ng/mL) for human and mouse plasma samples. Mouse tumor tissue samples required the use of a calibration curve prepared in the same matrix due to the lower recovery of 40% from this matrix. Then, accuracy and precision were within the generally accepted range of ±15% for bioanalytical assays. Ko143 was stable in human plasma for up to 3 repeated freeze–thaw cycles and when stored at room temperature for up to 72 h. However, when kept at room temperature in mouse plasma, Ko143 was rapidly degraded by esterase activity, which could be prevented by collection of blood into sodium fluoride-containing tubes and maintaining samples on ice during pretreatment. A preliminary pharmacokinetics study in mice demonstrated the applicability of this assay for ABCG2 resistance studies *in vivo*.

1. Introduction

Fumitremorgin C (FTC) was the first potent ABCG2 inhibitor identified in a cell-based transport screen [1,2]. ABCG2 is a member of the G group of ATP-binding cassette (ABC) transporters that can efflux a wide variety of compounds, including the topoisomerase I inhibitor topotecan [3]. ABCG2 is expressed in the apical plasma membrane of hepatocytes, kidney, intestinal and mammary epithelial cells, where it plays a critical role in drug disposition. Endothelial expression of ABCG2 in the blood–brain, blood–testis and maternal–foetal barriers contributes to the protection against xenobiotics [4]. Previously, it was shown that ABCG2 was responsible for acquired topotecan resistance in our BRCA1-deficient mouse model of hereditary breast cancer [5]. To test if this topotecan resistance can be overcome by inhibition of ABCG2, we are now testing the combination of topotecan therapy with the FTC analogue Ko143.

The *in vivo* neurotoxicity of the mycotoxin FTC stimulated the search for analogues with reduced toxicity profiles [6]. Of these, Ko143 was the most potent and specific inhibitor, increasing oral topotecan availability 4–6-fold at a dose of 10 mg per kg body weight in *Abcb1a/b* knockout mice. Ko143 is the most widely used ABCG2 inhibitor in experimental models and to optimize its use *in vivo*, it is essential to study its pharmacokinetic behaviour. This knowledge is also helpful to guide development of next generation ABCG2 inhibitors [7,8].

In contrast to FTC [9], no bioanalytical assays are available for Ko143. Here, we report a validated reversed-phase high-performance liquid chromatography method for the quantification of Ko143 concentrations in human and mouse plasma as well

* Corresponding author. Tel.: +31 020 512 2792; fax: +31 020 512 2799.
E-mail address: o.v.tellingen@nki.nl (O. van Tellingen).

1570-0232/$ – see front matter © 2012 Elsevier B.V. All rights reserved.
http://dx.doi.org/10.1016/j.jchromb.2012.11.003

as in mouse tumor homogenates. Based on an *in vitro* EC_{90} concentration of 12 ng/mL from previous reports [6,10,11], we aimed to measure Ko143 concentrations of at least 10 ng/mL to perform a preliminary pharmacokinetics experiment. Instead of the UV detection method used by Garimella et al. [9] for FTC, we developed a more selective and sensitive fluorescence-based approach that allowed accurate quantification of Ko143 down to 2 ng/mL (the lower limit of quantification), using FTC as internal standard and diethyl ether liquid–liquid extraction for sample pretreatment.

2. Experimental

2.1. Chemicals and reagents

Ko143 was purchased from Tocris Bioscience (Minneapolis, MN, USA). The reference Ko143 [6] for mass spectrometry analysis was a kind gift from Dr. Alfred H. Schinkel. Roquefortine C was purchased from BioAustralis Fine Chemicals (Smithfield, NSW, Australia). Fumitremorgin C and diethyl ether were purchased from Sigma–Aldrich (St. Louis, MO, USA). Acetonitrile originated from Biosolve (Valkenswaard, The Netherlands), methanol from Merck (Darmstadt, Germany) and fraction V bovine serum albumin (BSA) from Roche (Mannheim, Germany). Water was purified by the Milli-Q Plus system (Millipore, Milford, USA). Drug-free human plasma was obtained from healthy donors from the Central Laboratory of the Blood Transfusion Service (Sanquin, Amsterdam, The Netherlands).

2.2. Instrumentation and chromatographic separation

The chromatographic system consisted of a model SRD-3600 Solvent Racks (with in-line degasser), a model DGP-3600A pump, a model WPS-3000TSL autosampler (Dionex, Sunnyvale, CA, USA), and a FP-1510 fluorescence detector (Jasco, Hachioji City, Japan) with excitation and emission wavelengths set at 295 nm and 350 nm, respectively. Some initial experiments were carried out using a model 996 UV-photodiode array (UV-PDA) detector (Waters, Milford, MA, USA). Chromatographic separations were achieved using a stainless steel analytical GraceSmart RP18 column (2.1 mm × 150 mm) packed with 5 μm C18 material preceeded by a guard column (AJ0-A286 C18 cartridge; Phenomenex, Torrance, CA, USA). The mobile phase was prepared by mixing 620 mL of methanol with 380 mL of 10 mM ammonium acetate buffer pH 5.0. The mobile phase was delivered at a flow rate of 0.2 mL/min. Peak detection and integration was performed with a Chromeleon data system version 6.8 (Dionex, Sunnyvale, CA, USA).

2.3. Collection of blank murine specimens

Mice were housed and handled according to the institutional guidelines complying with Dutch legislation. Animals were kept in a temperature-controlled environment with a 12 h light/12 h dark cycle and received a standard diet (AM-II, Hope Farms, Woerden, The Netherlands) and acidified water *ad libitum*. Adult female *Abcg2*$^{-/-}$ FVB/N mice (at least eight weeks of age [12]) were anesthetized with isoflurane and whole blood samples were obtained by cardiac puncture and collected in heparin- or sodium fluoride-containing tubes. Next, the mice were killed by cervical dislocation and the tumors dissected. Blood was centrifuged (5 min, 4000 rpm, 4 °C) to separate the plasma fraction and both plasma and tumor samples were stored at −20 °C. Frozen mouse tumors were thawed at 4 °C and homogenized 1:5 in 1% (w/v) BSA in water (equivalent to 500 mg tumor in 2.5 mL volume) using a FastPrep-24 high speed bench top homogenizer (MP-Biomedicals, Santa Ana, CA, USA) at 6.0 M/s for 30 s in 4.5 mL tubes. Homogenized samples were stored at −20 °C until analysis.

2.4. Drug stock solutions and internal standard

Ko143 powder was accurately weighed and dissolved in dimethyl sulfoxide (DMSO) to yield three independent stocks of 1.283, 1.230 and 1.497 mg/mL. This first stock solution was used to prepare a 500 ng/mL calibration stock standard in blank human plasma. The structurally very similar FTC was used as internal standard (IS) and 1 mg/mL FTC stock solution was prepared in DMSO. A working solution of IS was prepared in advance by 10,000-fold diluting the stock in acetonitrile–water (20:80, v/v), to yield a final concentration of 100 ng/mL. Calibration stock and IS stock solution were aliquoted and stored at −20 °C.

2.5. Calibration standards and quality control samples

Calibration standards for the determination of Ko143 in human and mouse plasma were prepared in blank human plasma at nominal concentrations of 1.026, 2.053, 5.13, 10.26, 20.53, 51.3, 102.6, 205.3 and 513 ng/mL, whereas calibration standards for mouse tumor determinations were prepared in mouse tumor homogenate. The standards were freshly prepared for each analytical run and analyzed in duplicate. Quality control samples were prepared by appropriate dilution of independent stocks in human plasma and mouse plasma and tumor homogenate to final concentrations of 9.84, 49.2, 246 and 2460 ng/mL of Ko143.

2.6. Sample pretreatment

Sample pretreatment involved liquid–liquid extraction. Samples that were found to contain a Ko143 concentration above the upper limit of quantification (ULQ) were diluted 10-fold with blank human plasma and re-assayed. A volume of 100 μL of plasma or tissue homogenate was pipetted into a 2 mL polypropylene tube (Eppendorf, Hamburg, Germany). Volumes of 50 μL of the 100 ng/mL internal standard stock solution and 1 mL diethyl ether were added. After vigorously mixing for 5 min, the samples were centrifuged for 3 min at 5000 g to separate the aqueous and organic layers. The aqueous layer was frozen by placing the vial in a dry ice/ethanol bath. The upper organic layer was decanted into a 1.5 mL micro tube (Brand, Wertheim, Germany). After evaporation in a Speed-Vac SC210A (Savant, Farmingdale, NY, USA) at 43 °C, the residue was reconstituted in 200 μL acetonitrile–water (20:80, v/v) by vigorous vortexing for 10 seconds and sonication for 5 min. The sample was then briefly vortexed again, centrifuged and placed in the autosampler.

2.7. Assay validation

Validation of the assay including the determination of the linearity, precision, accuracy, selectivity, lower limit of quantification, recovery and stability was first completed in human plasma and next in murine plasma and tumor homogenate following the guidelines of the FDA (Food and Drug Administration Bioanalytical Method Validation 2001). The statistical analysis was done with the software package SPSS (SPSS Statistics Release 17.0, Chicago, IL, USA).

2.8. Linearity and sensitivity

Calibration curves were calculated by linear regression analysis of the peak area ratios of Ko143 to IS *versus* the concentration of Ko143. We first established the most appropriate weight factor as $1/x^2$ (reciprocal of the square of the concentration). The *F*-test

for lack of fit ($\alpha = 0.05$) was used to evaluate the linearity of the calibration curves.

2.9. Precision and accuracy

To assess the accuracy, within-day and between-day precisions of the assay, we performed $N = 6$ replicate measurements of the quality control samples in human plasma (10, 50 and 250 ng/mL Ko143) in 3 different analytical runs. We also assessed the accuracy and within-day precision of the assay in murine matrices, namely, mouse plasma and tumor homogenates spiked with 10, 50 and 250 ng/mL Ko143 in triplicate for each spiked concentration in one analytical run.

The between-groups mean square ($MS_{between\text{-}day}$), within-groups mean square ($MS_{within\text{-}day}$) and the grand mean (GM) of the observed concentrations across runs were calculated using SPSS. The standard deviation of each run (SD_{run}), BDP% (between-day precision) and the WDP% (within-day precision) were calculated using the formulas:

$$SD_{run} = \left[\frac{MS_{between} - MS_{within}}{N}\right]^{1/2}$$

where N represents the number of replicates within each run.

$$BDP\,\% = \left[\frac{SD_{run}}{GM}\right] \times 100\%$$

$$WDP\,\% = \left[\frac{MS_{within\text{-}day}^{1/2}}{GM}\right] \times 100\%$$

The accuracy was expressed as the mean percentage deviation (DEV%) calculated by:

$$DEV\,\% = \left[\frac{GM\ observed\ concentration - nominal\ concentration}{nominal\ concentration}\right] \times 100\%$$

Values within ±15% for precision and accuracy were considered acceptable.

2.10. Selectivity

To assess the selectivity of the assay, drug-free human plasma from six healthy donors and mouse plasma and tissues from untreated mice were processed and analyzed to determine whether endogenous peaks co-eluted with Ko143 or the internal standard. All prepared solutions were directly analyzed under the chromatographic conditions described above.

2.11. Determination of the lower limit of quantification

Lower limit of detection (LOD) was defined as the peak height that was five times larger than baseline signal-to-noise. To validate the lower limit of quantification (LLQ), human plasma spiked with 2 different concentrations (5 and 2 ng/mL) of Ko143 was processed and analyzed. The LLQ was accepted when the deviation of accuracy (DEV%) and precision were within the ±20% range.

2.12. Stability

The stability of Ko143 and FTC (internal standard) was examined in human plasma subjected to 0–3 freeze–thaw cycles, and in pretreated samples reconstituted in acetonitrile–water (20:80, v/v), kept at room temperature for a period of 0–24 h. Furthermore, we examined the stability and photosensitivity of Ko143 and FTC in human plasma for an extended period of up to 72 h under three different conditions: at room temperature exposed to ambient light conditions or protected from light, and at 4 °C. Stability

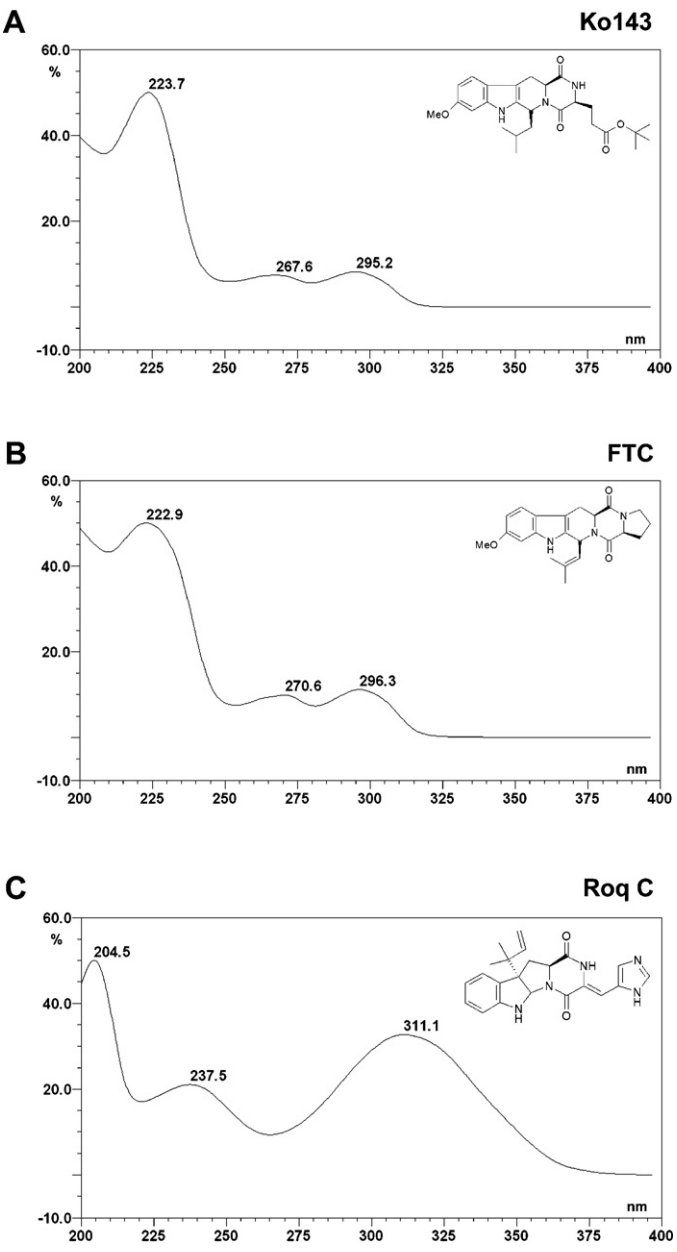

Fig. 1. UV spectra and chemical structures of Ko143 (A), fumitremorgin C (FTC, B) and roquefortine C (RoqC, C).

was assessed by comparing the Ko143 concentrations with those in freshly prepared and analyzed spiked samples. Long-term storage stability for up to one month at −20 °C was confirmed in human and mouse plasma, containing 250 and 2500 ng/mL Ko143.

2.13. Recovery

The recovery of sample pretreatment was calculated by comparing the peak area from spiked human and mouse matrices with those prepared from drug stock diluted in acetonitrile–water (20:80, v/v) at the same concentrations. Six samples at low, medium and high concentrations (10, 50 and 250 ng/mL Ko143) were analyzed.

2.14. Long-term reproducibility

After validation we used this assay to analyze mouse Ko143 pharmacokinetics. Reproducibility was established taking the

Table 1
Accuracy, within-day and between-day precision of Ko143 determination in human plasma, mouse plasma and mouse tumor homogenate spiked at nominal concentrations of 2460, 246.0, 49.2 and 9.84 ng/mL of Ko143. The presented human plasma data were acquired in three independent analytical runs with 6 replicates per concentration and run ($N = 18$). Accuracy and within-day precision of Ko143 determination in mouse plasma and tumor homogenate are based on freshly prepared samples, each assayed in 6 replicates ($N = 6$). The quality control samples containing 2460 ng/mL were diluted 10-fold with blank human plasma.

Specimen	Nominal concentration (ng/mL or ng/g)	Measured concentration (ng/mL or ng/g) (mean ± sd)	Accuracy (%)		Within-day Precision (%)	Between-day Precision (%)
Human plasma	2460.00	2299.51 ± 183.52	($N = 18$)	−6.52	7.00	4.56
	246.00	239.87 ± 12.68	($N = 18$)	−2.49	2.53	5.53
	49.20	47.56 ± 1.58	($N = 18$)	−3.34	1.34	3.62
	9.84	9.39 ± 0.45	($N = 18$)	−4.58	4.43	2.03
Mouse plasma	2460.00	2305.12 ± 92.01	($N = 6$)	−6.30		
	246.00	222.25 ± 8.25	($N = 6$)	−9.65		
	49.20	45.45 ± 1.34	($N = 6$)	−7.62		
	9.84	9.47 ± 0.29	($N = 6$)	−3.79		
Mouse tumor (human plasma calibration curve)	246.00	160.92 ± 2.69	($N = 6$)	−34.59		
	49.20	39.87 ± 1.83	($N = 6$)	−18.97		
	9.84	9.85 ± 0.33	($N = 6$)	0.10		
Mouse tumor (mouse tumor calibration curve)	246.00	253.55 ± 12.77	($N = 6$)	3.07		
	49.20	54.20 ± 2.23	($N = 6$)	10.16		
	9.84	10.93 ± 0.39	($N = 6$)	11.11		

Table 2
Determination and validation of the lower limit of quantification. Accuracy and within-day precision were assessed in human plasma spiked with 5 and 2 ng/mL Ko143.

Specimen	Nominal concentration (ng/mL)	Measured concentration (ng/mL) (mean ± sd)		Accuracy (%)	Within-day precision (%)	Between-day precision (%)
Human plasma	5.13	5.12 ± 0.28	($N = 14$)	<0.01	4.52	5.57
	2.05	2.01 ± 0.23	($N = 14$)	−0.02	11.53	8.47

Table 3
Stability of Ko143 in human plasma after three freeze–thaw cycles and in EDTA or NaF, stored at three different conditions for 72 h. The stability is expressed as the mean percentage deviation (DEV%).

Specimen	Nominal concentration (ng/mL)	Cycle 0 (mean ± sd)	Cycle 3 (mean ± sd)	DEV(%) Cycle 3–0	DEV (%) nominal
Human plasma	246.00	237.60 ± 4.18	218.87 ± 11.10	−7.88	3.41
	9.84	10.10 ± 0.95	10.33 ± 0.40	2.28	2.64

		Storage condition		Measured concentration (ng/mL) (mean ± sd)	DEV (%) nominal
Human plasma (EDTA)	246.00	0 h		244.74 ± 1.08	−0.51
		72 h			
			−4 °C, dark	277.36 ± 3.20	12.75
			RT, dark	253.64 ± 4.78	3.11
			RT, light	242.11 ± 5.43	−1.58
Human plasma (NaF)	246.00				
		72 h			
			−4 °C, dark	263.03 ± 8.32	6.92
			RT, dark	270.23 ± 8.00	9.85
			RT, light	261.30 ± 5.49	6.22
Human plasma (EDTA)	49.20	0 h		46.96 ± 1.08	−4.55
		72 h			
			−4 °C, dark	55.36 ± 0.39	12.52
			RT, dark	48.93 ± 1.03	−0.55
			RT, light	49.80 ± 0.75	1.22
Human plasma (NaF)	49.20				
		72 h			
			−4 °C, dark	54.42 ± 1.66	10.61
			RT, dark	53.72 ± 0.78	9.19
			RT, light	52.33 ± 0.49	6.36
Human plasma (EDTA)	9.84	0 h		9.73 ± 0.23	−1.12
		72 h			
			−4 °C, dark	10.82 ± 0.57	9.96
			RT, dark	10.07 ± 0.34	2.34
			RT, light	9.77 ± 0.25	−0.71
Human plasma (NaF)	9.84				
		72 h			
			−4 °C, dark	11.20 ± 0.13	13.82
			RT, dark	10.90 ± 0.42	10.77
			RT, light	10.95 ± 0.24	11.28

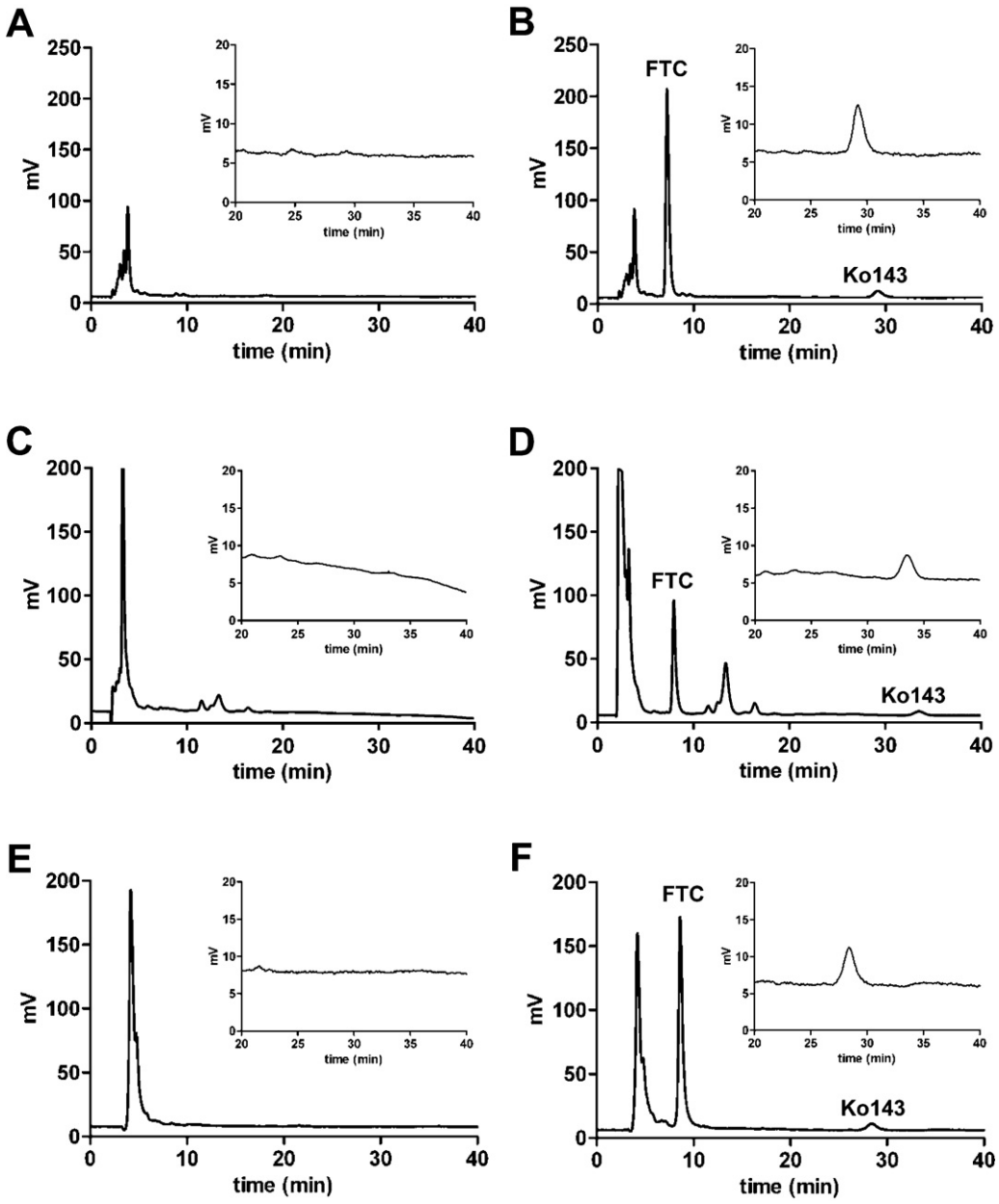

Fig. 2. Representative RP-HPLC chromatograms of fumitremorgin C and Ko143. The chromatograms of blank (A, C and E) and spiked (10 ng/mL Ko143, B, D and F) samples of human plasma (A and B), mouse plasma (C and D) and mouse tumor homogenate (E and F) are shown. Inserts show the location of the Ko143 peak to a different scale.

results of 7 runs over a period of about seven months. Within-day and between-day precision were calculated using a one-way ANOVA test (see above) for the quality control samples assayed in triplicate at 3 concentrations of 10, 50 and 250 ng/mL Ko143 within each analytical run.

2.15. In vivo applicability

To demonstrate the applicability of this assay for preclinical pharmacokinetics study purposes, we analyzed a series of murine plasma samples from an *in vivo* experiment. Ko143 was used by diluting 10 mg/mL DMSO stocks in 15% (w/v) 2-hydroxyl-propyl-β-cyclodextrine/PBS to a final concentration of 1 mg/mL. Animals were dosed with this solution at 10 mg per kg body weight by i.p. injection of 10 μL/g body weight. Blood was sampled by cardiac puncture at 15, 30, 60, 90 and 120 min after Ko143 administration from at least three adult *Abcg2*$^{-/-}$ FVB/N females (of at least eight weeks of age [12]) per time point. After collection, the blood samples were processed and stored as described in the section Collection of blank murine specimens. The initial analysis of the 15, 30 and 60 min plasma samples revealed that the measured Ko143 levels were above the linear dynamic range of the validated assay. We therefore re-analyzed these samples after 1:10 dilution in blank plasma.

3. Results and discussion

3.1. Chromatographic separation and detection mode

We started the optimization of the chromatographic analysis of Ko143 using a reversed phase C18 column in combination with UV detection, based on the method reported previously for FTC by Garimella et al. [9]. These authors proposed that their methodology might also be useful for the determination of Ko143, since they

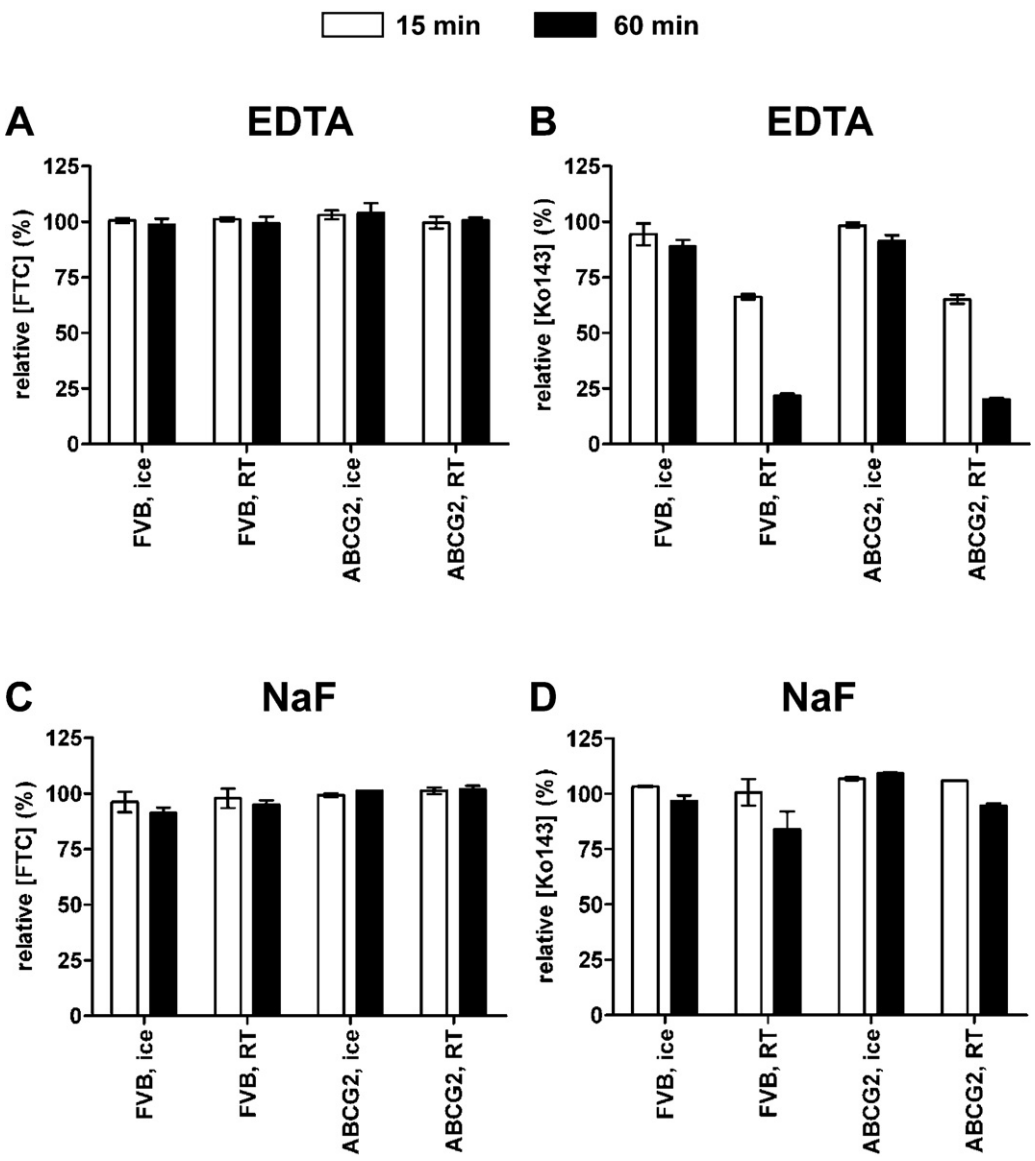

Fig. 3. Mouse plasma esterase-mediated degradation of Ko143. In contrast to fumitremorgin C, Ko143 contains an ester bond (Fig. 1A) that is sensitive to plasma esterase-mediated degradation. Plasma from FVB/N wildtype or *Abcg2*$^{-/-}$ mice was either collected into EDTA (A and B) or sodium fluoride (NaF, C and D) tubes and spiked with 100 ng/mL FTC (A and C) and Ko143 (B and D). Samples were kept at room temperature (RT) or on ice for 0, 15 and 60 min. Ko143 and FTC peak areas were determined by RP-HPLC and normalized to the initial peak area at the start of the experiment (%). Each sample was measured in duplo. Error bars indicate standard deviations.

observed a chromatographic peak following Ko143 injection into their HPLC system. However, we were unable to reproduce this result. We found that the absorbance spectra reported for Ko143 (and roquefortine C) in that study were incorrect. In fact, the UV spectra of FTC and Ko143 are very similar and quite distinct from roquefortine C (Fig. 1). Moreover, we observed that the retention time of Ko143 on C18 columns was much longer than of FTC, whereas the presumed peak in the study by Garimella et al. eluted before FTC. Thus, most likely, the compound detected by Garimella et al. was not Ko143. We confirmed that the mass spectra of our analytical Ko143, purchased from Tocris, were consistent with the empirical formula of elemental composition and identical to the reference Ko143, as published by Allen et al. [6] (Supplementary Fig. 1). Moreover, we also found that the selectivity and sensitivity at the optimal UV wavelength of 295 nm would probably not be sufficient to meet the required LLQ of 10 ng/mL of Ko143 in mouse plasma samples. Based on the chemical structures of Ko143, FTC and roquefortine C (Fig. 1), we decided to test whether these compounds have useful fluorescence properties. The parent compound FTC and its analogue Ko143 have three UV absorption peaks as can be deduced from the UV spectra in Fig. 1. We selected 295 nm as the excitation wavelength and acquired an excellent fluorescence yield at 350 nm, selected as the optimal emission wavelength. Roquefortine C, however, did not show satisfactory fluorescence properties under these conditions (Fig. 1C) and we therefore chose FTC as the internal standard for quantitative analysis.

3.2. Sample pretreatment and recovery

Mean recoveries from diethyl ether liquid–liquid extraction of human and mouse plasma samples were 50%. Despite this rather modest recovery, the diethyl ether extraction method was favoured because of its high selectivity and limited additional handling time per individual sample. This ensured efficient analysis of large sample sets and high reproducibility of the measurements. Only some minor chromatographic peaks were found in blank samples and following further optimization of the mobile phase composition,

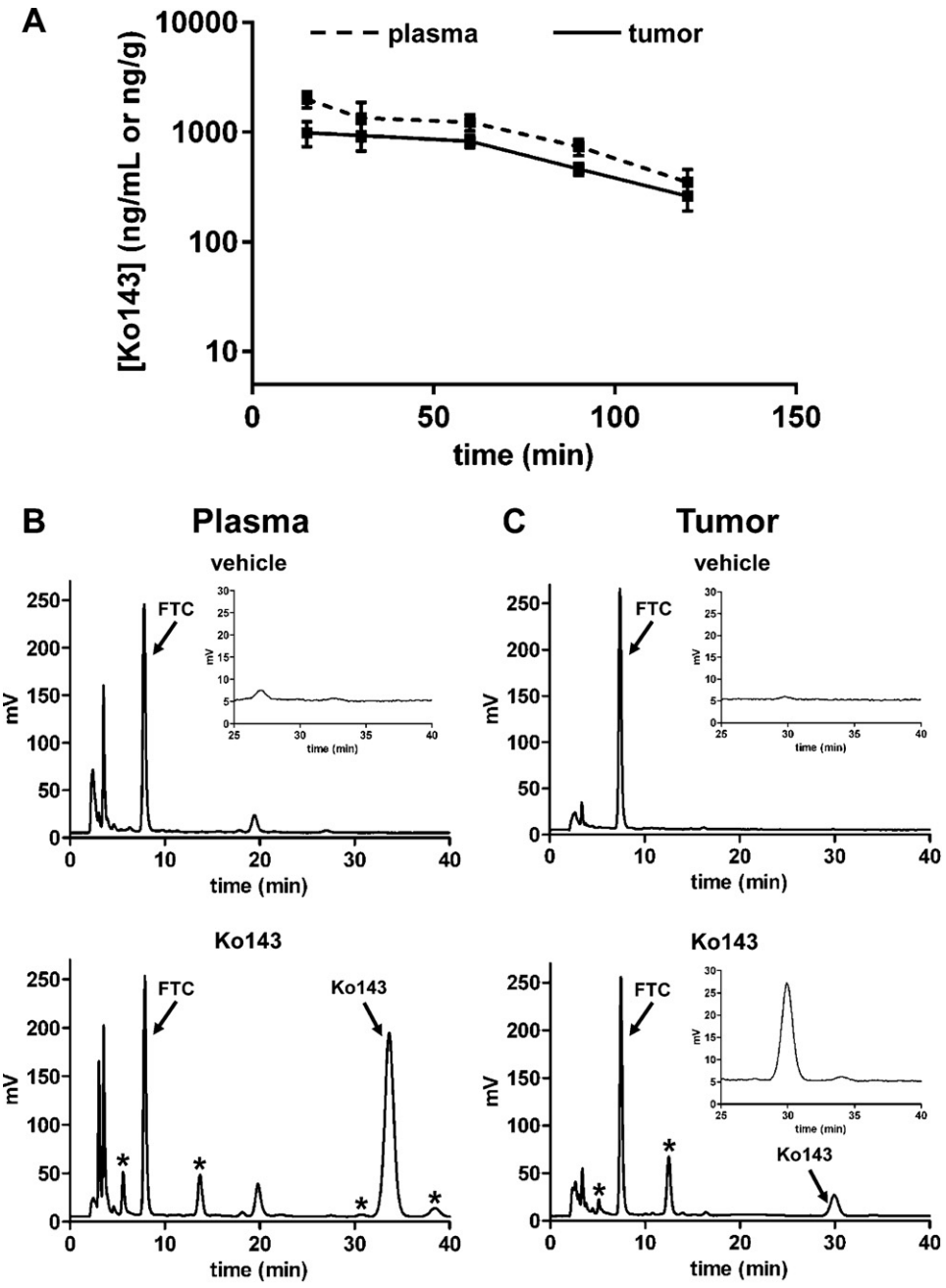

Fig. 4. Preliminary Ko143 pharmacokinetics in *Abcg2*$^{-/-}$ mice. Plasma (ng/mL) and tumor (ng/g) concentration – time curves of Ko143 (A). Ko143 was administered at a dose of 10 mg per kg body weight and samples were collected at 15, 30, 60, 90 and 120 min after i.p. injection. Error bars indicate standard deviations of at least three animals per time point. Representative RP-HPLC chromatograms of Ko143 in mouse plasma (undiluted, B) and tumors (C), 120 min after i.p. injection of vehicle (top) or Ko143 (bottom). Note that the Ko143 peak height difference between the plasma and tumor chromatograms is due to the 1:5 homogenization in 1% BSA prior to RP-HPLC analysis. Besides Ko143, there were several unknown peaks (*) present in the plasma and tumor chromatograms of animals that received Ko143 and that were not detected in the vehicle-treated mice. Inserts in (B) and (C) show the location of the Ko143 peak to a different scale.

blank human (Fig. 2A) and mouse plasma (Fig. 2C) did not contain endogenous substances that co-eluted with Ko143 or FTC. Similarly, mouse tumor homogenate was also free of interfering peaks (Fig. 2E). Sharp chromatographic peaks were obtained in all these matrices when Ko143 was spiked at 10 ng/mL (Fig. 2B, D and F). These results demonstrate that the selectivity of this assay was sufficient to allow quantification down to our initial aim of 10 ng/mL.

3.3. Accuracy and precision

The validation of the Ko143 analytical procedure was first completed in human plasma as this matrix could be easily obtained in relatively large quantities, in contrast to the biological matrices from mice. Accuracy and precision of Ko143 determinations in human plasma and mouse matrices using human plasma as matrix for the calibration samples are summarized in Table 1. At three different Ko143 concentrations (250, 50 and 10 ng/mL), acceptable accuracy of ±15% was achieved for both human and mouse plasma. Unfortunately, the results for spiked Ko143 at the same concentrations in mouse tumor homogenate were not within acceptable limits due to a lower recovery of 40% from this matrix. Consequently, we decided to prepare a separate set of calibration samples prepared in tumor matrix. By doing this we could also achieve in the spiked mouse tumor homogenates accuracy and precision within

the acceptable limits of ±15% (Table 1). Calibration curves were linear in three randomly selected analytical runs over the tested concentration range of 2–500 ng/mL and calculation by weighted ($1/x^2$) linear regression analysis yielded the best fit ($r > 0.99$).

The LLQ was established by spiking human plasma with 2 and 5 ng/mL Ko143. Accuracy, within-day and between-day precision requirements for the LLQ (±20%) were still met at 2 ng/mL (Table 2), making this concentration the LLQ of the assay.

3.4. Long-term reproducibility

Between-run and within-run precisions were determined for quality control samples at three Ko143 concentrations of 250, 50 and 10 ng/mL. These quality control samples were included among other samples in each analytical run and analyzed in duplicate during the routine use of this assay. The reproducibility or between-run precision was 5.5%, 3.6%, and 2.0%, respectively. The repeatability or within-run precision was 2.5%, 1.3% and 4.4%, respectively. Both reproducibility and repeatability fell within the ±15% limit and were therefore accepted for the different concentrations.

3.5. Stability and esterase sensitivity

Ko143 stability in human plasma was assessed in triplicate for up to three freeze–thaw cycles at 250 and 10 ng/mL (Table 3). Stability was evaluated by comparing the measured Ko143 concentrations with those in freshly prepared samples. As the deviations at both Ko143 levels were less than 15%, we concluded that repeated freeze–thaw cycles did not significantly affect the stability of this compound. Similarly, human and mouse plasma samples containing 250 and 2500 ng/mL Ko143 were found to be stable for at least one month when stored at −20 °C.

However, when we analyzed mouse plasma quality control samples that were kept at room temperature during pretreatment, we found that the Ko143 levels were much lower than expected and even further decreased upon re-analysis (data not shown). Based on the ester bond in the molecule (Fig. 1A), we hypothesized that esterase activity in mouse plasma could be responsible for this Ko143 degradation. To test this, we spiked mouse plasma samples with 100 ng Ko143 per mL and kept these for 15 and 60 min on ice or at room temperature, before measuring the Ko143 levels (Fig. 3). Plasma samples were either from FVB/N wildtype or *Abcg2*$^{-/-}$ animals and prepared from blood collected into EDTA or sodium fluoride (NaF) tubes. In contrast to the internal standard FTC (Fig. 3A and C), relative Ko143 levels (%) dramatically decreased over time when both wildtype and *Abcg2*$^{-/-}$ EDTA plasma samples were kept at room temperature, but not on ice (Fig. 3B). The Ko143 degradation at room temperature could be prevented by addition of sodium fluoride to the collection tubes (Fig. 3D). No additional peaks emerged in the chromatogram during degradation.

Based on this knowledge of esterase sensitivity, we re-checked the stability of Ko143 in human plasma under three different storage conditions (Table 3). We found that the stability in human plasma was much better than in mouse plasma. Although the results of the EDTA-containing samples were still acceptable, the sodium fluoride-containing samples were more consistent. This argues in favour of using this esterase inhibitor also for human plasma samples.

3.6. In vivo applicability

A preliminary Ko143 pharmacokinetics experiment in *Abcg2*$^{-/-}$ mice demonstrated the applicability of this assay *in vivo*. Following a dose of 10 mg per kg body weight, plasma and tumor Ko143 levels were measured over a time course of 15–120 min (Fig 4A). As a result, we found that Ko143 concentrations in both matrices were well above the LLQ of the assay and the previously reported EC_{90} of 12 ng/mL [6], at least within the time frame of this experiment. Compared with the vehicle-treated animals, several additional peaks of unknown substances were detected next to the Ko143 peak in the chromatograms of plasma (Fig. 4B) and tumor (Fig. 4C) samples from the Ko143-treated animals. These peaks may represent potential Ko143 metabolites, but other experimental approaches like mass spectrometry are needed to identify these substances.

4. Conclusions

Here, we have validated a sensitive and selective method to quantify Ko143 levels in human and mouse plasma as well as mouse tumor homogenates. Esterase-mediated degradation of Ko143 in mouse plasma could be circumvented by collection of blood samples into sodium fluoride tubes and performing sample pretreatment on ice. Recovery of Ko143 from mouse tumor homogenate (40%) was lower than from human or mouse plasma (50%). When quantifying Ko143 levels in this matrix, calibration and quality control samples in the same matrix have to be included in the analytical run. A preliminary pharmacokinetics experiment showed that effective Ko143 levels were reached when animals were dosed at 10 mg per kg body weight. This Ko143 assay is currently used to evaluate Ko143 + topotecan combination therapy in mice, bearing BRCA1-deficient mammary tumors that acquired resistance to topotecan by increasing ABCG2 levels.

Acknowledgements

We thank Sven Rottenberg for providing the Ko143 and Piet Borst and Koen van de Wetering for critical reading of the manuscript. We acknowledge Robert S. Jansen for the mass spectrometry analysis of Ko143.

Appendix A. Supplementary data

Supplementary data associated with this article can be found, in the online version, at http://dx.doi.org/10.1016/j.jchromb.2012.11.003.

References

[1] S.K. Rabindran, H. He, M. Singh, E. Brown, K.I. Collins, T. Annable, L.M. Greenberger, Cancer Res. 58 (1998) 5850.
[2] S.K. Rabindran, D.D. Ross, L.A. Doyle, W. Yang, L.M. Greenberger, Cancer Res. 60 (2000) 47.
[3] R.W. Robey, K.K. To, O. Polgar, M. Dohse, P. Fetsch, M. Dean, S.E. Bates, Adv. Drug Deliv. Rev. 61 (2009) 3.
[4] M.L. Vlaming, J.S. Lagas, A.H. Schinkel, Adv. Drug Deliv. Rev. 61 (2009) 14.
[5] S.A. Zander, A. Kersbergen, E. van der Burg, N. de Water, O. van Tellingen, S. Gunnarsdottir, J.E. Jaspers, M. Pajic, A.O. Nygren, J. Jonkers, P. Borst, S. Rottenberg, Cancer Res. 70 (2010) 1700.
[6] J.D. Allen, A. van Loevezijn, J.M. Lakhai, M. van der Valk, O. van Tellingen, G. Reid, J.H. Schellens, G.J. Koomen, A.H. Schinkel, Mol. Cancer Ther. 1 (2002) 417.
[7] C.J. Henrich, R.W. Robey, H.R. Bokesch, S.E. Bates, S. Shukla, S.V. Ambudkar, M. Dean, J.B. McMahon, Mol. Cancer Ther. 6 (2007) 3271.
[8] H. Peng, Z. Dong, J. Qi, Y. Yang, Y. Liu, Z. Li, J. Xu, J.T. Zhang, PLoS ONE 4 (2009) e5676.
[9] T.S. Garimella, D.D. Ross, K.S. Bauer, J. Chromatogr. B: Analyt. Technol. Biomed. Life Sci. 807 (2004) 203.
[10] J.D. Allen, R.F. Brinkhuis, J. Wijnholds, A.H. Schinkel, Cancer Res. 59 (1999) 4237.
[11] M. Maliepaard, M.A. van Gastelen, L.A. de Jong, D. Pluim, R.C. van Waardenburg, M.C. Ruevekamp-Helmers, B.G. Floot, J.H. Schellens, Cancer Res. 59 (1999) 4559.
[12] J.W. Jonker, M. Buitelaar, E. Wagenaar, M.A. van der Valk, G.L. Scheffer, R.J. Scheper, T. Plosch, F. Kuipers, R.P. Elferink, H. Rosing, J.H. Beijnen, A.H. Schinkel, Proc. Natl. Acad. Sci. U.S.A. 99 (2002) 15649.